Optimization of the monolayer growth in adsorption-desorption processes

S. Živković,[1] Z. M. Jakšić,[1] I. Lončarević,[2] Lj. Budinski-Petković,[2] S. B. Vrhovac,[1,*] and A. Belić[1]
[1]*Institute of Physics Belgrade, University of Belgrade, Pregrevica 118, Zemun 11080, Belgrade, Serbia*
[2]*Faculty of Engineering, Trg D. Obradovića 6, Novi Sad 21000, Serbia*
(Received 4 July 2013; revised manuscript received 23 October 2013; published 22 November 2013)

Kinetics of the deposition process of dimers in the presence of desorption is studied by Monte Carlo method on a one-dimensional lattice. The aim of this work is to investigate how do various temporal dependencies of the desorption rate hasten or slow down the deposition process. The growth of the coverage $\theta(t)$ above the jamming limit to its steady-state value θ_∞ is analyzed when the desorption probability $P_{\rm des}$ decreases both stepwise and linearly (continuously) over a certain time domain. We report a numerical evidence that the time needed for a system to reach the given coverage θ can be significantly reduced if $P_{\rm des}$ decreases in time. Finally, a self-consistent optimization procedure, when the probability $P_{\rm des}$ depends on the current coverage density $\theta(t)$, is formulated and tested. The present model reproduces qualitatively the densification kinetics and the memory effects of vibrated granular materials. Our results suggest that the process of vibratory compaction of granular materials can be optimized by using a time dependent intensity of external excitations.

DOI: 10.1103/PhysRevE.88.052131 PACS number(s): 05.40.−a, 68.43.Mn, 68.43.Nr, 05.10.Ln

I. INTRODUCTION

Over the past two decades considerable scientific effort has been devoted to the development and understanding of the random sequential adsorption (RSA) model [1–3]. In RSA processes particles are randomly, sequentially, and irreversibly deposited onto a substrate. The dominant effect in RSA is the blocking of the available substrate area since the particles are not allowed to overlap. Within a monolayer deposit, each adsorbed particle affects the geometry of all later placements. If the adsorbed particles are permanently fixed at their spatial positions, the deposition process ceases when all unoccupied spaces are smaller than the size of an adsorbing particle. The system is then jammed in a nonequilibrium disordered state for which the limiting (jamming) coverage $\theta_{\rm jam}$ is less than the corresponding density of the closest packing. The kinetic properties of a deposition process are described by the time evolution of the coverage $\theta(t)$, which is the fraction of the substrate area covered by the adsorbed particles. On the basis of the nature of the substrate, the RSA models are broadly classified into continuum models and lattice models. The approach to the jamming coverage $\theta_{\rm jam}$ is known to be asymptotically algebraic for continuum systems [4–7] and exponential for the lattice models [8–12].

The possibility of desorption makes the process reversible and the system ultimately reaches an equilibrium state when the rate of desorption events becomes comparable to the rate of adsorption events. The density of particles in the steady state depends only on the desorption or adsorption rate ratio [13,14]. The approach of the coverage to its equilibrium value is very slow for low desorption probabilities. For the adsorption-desorption processes on a one-dimensional lattice a stretched exponential approach toward the steady state value of the coverage was found [15], while in two dimensions the Mittag-Leffler function gave a very good agreement with the simulation results for objects of various shapes [16].

Recently, interest in the field has expanded towards the modeling of the densification kinetics and other features of weakly vibrated granular materials [17–20]. The phenomenon of granular compaction involves the increase of the density of a granular medium subjected to shaking or tapping. The underlying dynamics is a subject of great interest in recent years [21]. Experiments have shown that when a granular material is submitted to vertical vibration or tapping, it slowly approaches a steady state of higher packing fraction [22–26]. The final steady state density is a decreasing function of the vibration intensity [26]. The relaxation dynamics is extremely slow, taking many thousands of taps to approach the steady state, and it slows down for lower vibration intensities.

Geometric exclusion effects characteristic for granular materials can be taken into account by reversible RSA, or adsorption-desorption processes. The adsorption-desorption model describes the kinetics of densification of a given layer of the granular material, perpendicular to the tapping force. As a result of a tapping event, particles leave the layer at random. On the other hand, they fall back into the layer under the influence of gravity, filling the opened empty locations and making the layer more compact in time. In the model, the ratio of desorption to adsorption rate $K = k_-/k_+$ plays a role similar to the vibration intensity Γ in real experiments [17].

Within the framework of the adsorption-desorption model it was shown in [18] that the increase of packing fraction can be accelerated by changing the desorption rate during the adsorption-desorption process. Actually, the problem of how various time dependencies of the desorption rate hasten or slow down the deposition process was formulated by Talbot and co-authors [18]. The determination of the optimum densification strategy, which has significant applications to vibratory compaction of granular materials, is still an open problem. The aim of this work is to investigate the way that the temporal dependence of the ratio $K = k_-/k_+$ influences the slow dynamics of deposition.

Here we present the results of extensive numerical simulations of the reversible RSA of dimers on the one-dimensional (1D) lattice. First, we focus on the process of reversible RSA with a constant value of desorption probability and determine

*vrhovac@ipb.ac.rs; http://www.ipb.ac.rs/~vrhovac/

the minimal time needed for a system to reach the given coverage $\theta > \theta_{\rm jam}$. The possibility to hasten the dynamics of reversible RSA is studied by decreasing the desorption probability in time. We report a numerical evidence that both stepwise and linear decay in the desorption probability over a certain time domain may be used to enhance the packing efficiency. In addition, we develop and analyze a self-consistent optimization protocol of deposition in which the optimal value of the desorption probability $P_{\rm des}$ is determined by the current coverage fraction $\theta(t)$. This work provides a closer insight into the deposition process with a time-varying desorption rate. Our model is a lattice based model, and in this sense it is not a realistic microscopic model of granular materials, but it does reproduce the complex phenomenology of granular media. Our results suggest that the process of vibratory compaction of granular materials can be optimized by using a time dependent vibration intensity.

The paper is organized as follows: Section II describes the details of the simulations. We give the simulation results and discussions in Sec. III. Finally, Sec. IV contains some additional comments and final remarks.

II. SIMULATION METHOD

The Monte Carlo simulations of adsorption-desorption processes are performed on a one-dimensional lattice of size $L = 10^5$ with a periodic boundary condition. The adsorbing objects are dimers covering two sites. Adsorption and desorption attempts are statistically independent and they perform sequentially with corresponding probabilities. The time t is counted by the number of adsorption attempts and scaled by the total number of lattice sites L. The data are averaged over 100 independent runs.

At each Monte Carlo step adsorption is attempted with probability P_a and desorption with probability $P_{\rm des}$. In the case of adsorption-desorption processes the kinetics is governed by the ratio of desorption to adsorption probability $P_{\rm des}/P_a$ [13,15,27]. Since we are interested in the ratio $P_{\rm des}/P_a$, in order to save computer time, it is convenient to take the adsorption probability to be $P_a = 1$. For each of these processes a lattice site is selected at random. In the case of adsorption, we try to place the dimer with the beginning at the selected site, i.e., we search whether adjacent site in a randomly chosen direction is unoccupied. If so, we place the dimer. Otherwise, we reject the deposition trial. When the attempted process is desorption, and if the selected site is occupied by a dimer, the object is removed from the lattice.

Here we consider the case of rapid adsorption and slow desorption ($P_{\rm des}/P_a \ll 1$). Then there exist two time scales controlling the evolution of the coverage $\theta(t)$. The first stage of the process is dominated by adsorption events and the kinetics displays an RSA-like behavior. With the growth of the coverage the desorption process becomes more and more important. Increasing the coverage $\theta(t)$ over the jamming limit $\theta_{\rm jam}$ is possible only due to the collective rearrangement of the adsorbed particles in order to open a hole large enough for the adsorption of an additional particle. We are interested in the time evolution of the coverage $\theta(t)$ in this later, postjamming time range.

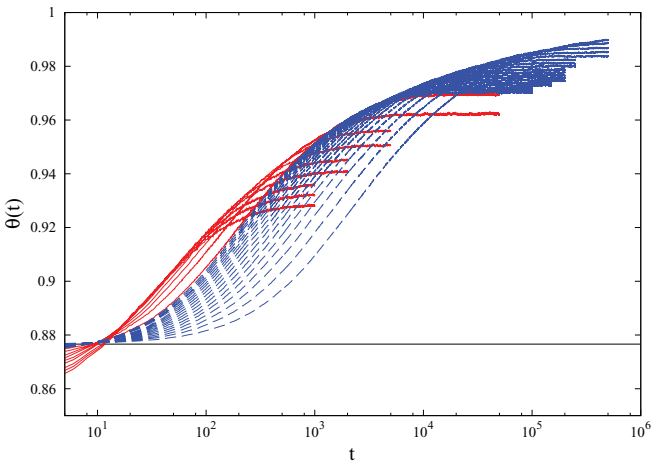

FIG. 1. (Color online) Temporal behavior of the coverage $\theta(t)$ for various desorption probabilities $P_{\rm des}$. Red (solid) lines correspond to values $P_{\rm des} = 0.010 + n \cdot 0.005$, $n = 0,1,2,\ldots,8$. Blue (dashed) lines correspond to values $P_{\rm des} = 0.0010 + n0.0005$, $n = 0,1,2,\ldots,17$. The equilibrium coverage θ_{eq} is found to decrease with the desorption probability $P_{\rm des}$. The horizontal line represents the jamming coverage for dimers, $\theta_{\rm jam} = 0.8766$.

III. RESULTS

Simulations of the adsorption-desorption processes of dimers were performed for a wide range of desorption probabilities $P_{\rm des} = 0.001$–0.050. In Fig. 1 the coverage is plotted as a function of time for different values of $P_{\rm des}$. Notice that the curves for different values of $P_{\rm des}$ always cross. This means that, for the reversible RSA model, the coverage is not always monotonic in $P_{\rm des}$. In Fig. 1, for example, the system with $P_{\rm des} = 0.030$ has a higher coverage than the system with $P_{\rm des} = 0.010$ for $15 \lesssim t \lesssim 500$; above $t \approx 500$ coverage is higher for the lower value of desorption probability, $P_{\rm des} = 0.010$. As already discussed in the context of the parking lot model [18], the existence of a minimum in the insertion probability (the fraction of the substrate that is available for the insertion of a new particle) is a sufficient condition for this phenomenon. It follows that for a given finite time, the densification can be made more efficient by changing the desorption probability $P_{\rm des}$ during the deposition process.

The first important step is to determine the desorption probability $P_{\rm des}(\theta)$ for which the time needed for a system to reach a given coverage $\theta > \theta_{\rm jam}$ is minimal. On the basis of the results presented in Fig. 1, we have examined the dependence of the time t_θ needed for a system to reach the given coverage $\theta > \theta_{\rm jam}$ on the desorption probability $P_{\rm des}$. These results are summarized in Fig. 2, where we show the time t_θ as a function of the desorption probability $P_{\rm des}$ for several coverage fractions θ. The linear trends at sufficiently low desorption probabilities $P_{\rm des}$ in Fig. 2 show that the time $t_\theta(P_{\rm des})$ starts to follow a power-law behavior, $t_\theta(P_{\rm des}) = A(\theta)\, P_{\rm des}^{-\gamma}$. The exponent γ remains nearly constant, $\gamma = 0.892 \pm 0.005$, regardless of the value of the coverage fraction θ. When coverage θ increases, this power-law behavior is restricted to smaller and smaller desorption probabilities $P_{\rm des}$. For each coverage $\theta > \theta_{\rm jam}$, a nonmonotonic $P_{\rm des}$ dependence is observed for the curve $t_\theta(P_{\rm des})$; it goes through a minimum $t_\theta^{\rm min}$ and tends to definite

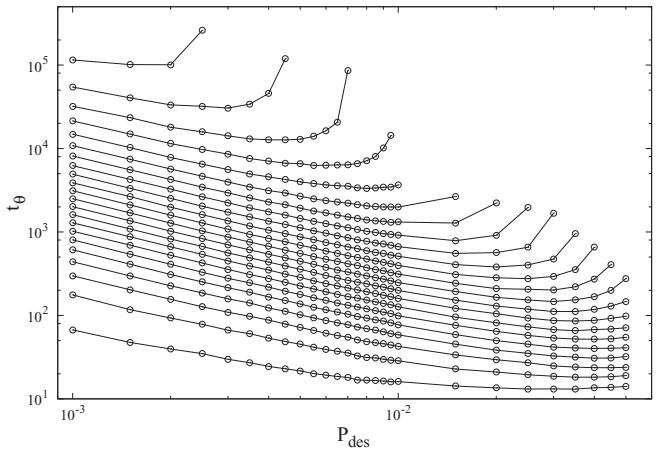

FIG. 2. The time t_θ needed for a system to reach the given coverage $\theta > \theta_{jam}$ depends on the value of desorption probability P_{des}. From bottom to top, lines $t_\theta = t_\theta(P_{des})$ correspond to coverages $\theta = 0.880 + n0.005$, $n = 0,1,2,\ldots,21$.

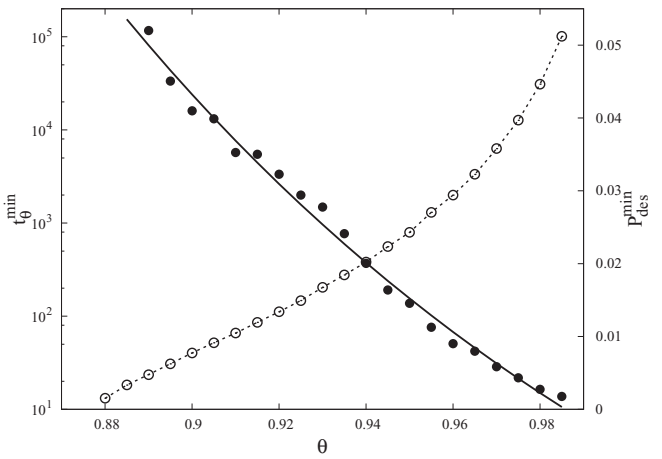

FIG. 3. Plot of the minimal time t_θ^{min} (empty circles) needed for a system to reach the given coverage θ in the reversible deposition process with a constant value of desorption probability $P_{des}^{min}(\theta)$. The full circles are plotted against the right-hand axis and give the probabilities $P_{des}^{min}(\theta)$ needed for a system to reach the given coverage θ in the shortest period of time t_θ^{min}. The solid superimposed line (right axis) represents the exponential fit of the form $P_{des}^{min}(\theta) = P_1 + P_2\exp(-\lambda\theta)$, with $P_1 = -5.915 \times 10^{-2}$, $P_2 = 32.30$, and $\lambda = 6.393$.

value which corresponds to the time needed for a system to reach the coverage θ, but as the equilibrium coverage θ_∞ for an appropriate value of P_{des}. Determined values for the equilibrium coverage θ_∞, resulting from the reversible RSA of dimers onto a 1D lattice, are given in Table I. Figure 3 allows us to determine the minimal time t_θ^{min} needed for a system to reach a given coverage $\theta > \theta_{jam}$ in the process of reversible RSA with the constant value of desorption probability $P_{des}^{min}(\theta)$. In the same figure, probabilities $P_{des}^{min}(\theta)$ needed for the system to reach a given coverage θ in the shortest period of time t_θ^{min} are displayed.

The purpose of this paper is to extend the analysis described above to the deposition processes in which the desorption probability P_{des} changes in time. We address the following questions: (1) How does the temporal dependence of the probability P_{des} influence the slow dynamics of deposition? (2) What is the optimum densification strategy, i.e., how do various time dependencies of the probability P_{des} hasten or slow down the deposition process? Our approach can provide some answers to such questions. In the next section it will be shown that the time needed for a system to reach a given coverage θ can be reduced if P_{des} decreases in time.

TABLE I. Equilibrium coverage fraction θ_∞ for various desorption probabilities P_{des}.

P_{des}	θ_∞	P_{des}	θ_∞
0.0010	0.9882	0.0080	0.9728
0.0015	0.9876	0.0085	0.9719
0.0020	0.9864	0.0090	0.9710
0.0025	0.9851	0.0095	0.9701
0.0030	0.9836	0.0100	0.9694
0.0035	0.9823	0.0150	0.9622
0.0040	0.9809	0.0200	0.9561
0.0045	0.9798	0.0250	0.9510
0.0050	0.9786	0.0300	0.9453
0.0055	0.9777	0.0350	0.9409
0.0060	0.9765	0.0400	0.9355
0.0065	0.9756	0.0450	0.9319
0.0070	0.9744	0.0500	0.9279
0.0075	0.9738		

A. Stepwise decrease of the desorption probability P_{des}

In the following, the possibility to hasten the dynamics of reversible RSA is studied by decreasing the desorption probability from $P_{des}^{(I)} = 0.050$ to $P_{des}^{(F)} = 0.010$ in a stepwise manner. Starting from an empty lattice, the system evolves at fixed desorption probability $P_{des}^{(I)} = 0.050$ up to the coverage $\theta^{(I)}$ above the jamming coverage θ_{jam}. Then, the desorption probability is abruptly lowered at fixed time intervals Δt_c. Those time intervals follow each other directly without any gap. We always use an instantaneous drop of $\Delta P_{des} = 0.005$ for a change of the desorption probability P_{des}, so that the final probability of $P_{des}^{(F)} = 0.010$ is reached after eight abrupt changes of P_{des}. The final desorption probability $P_{des}^{(F)}$ does not change further in time.

In Fig. 4, we demonstrate that the deposition process can be made much more efficient by decreasing the desorption probability P_{des} in time. Here, the time dependence of the coverage $\theta(t)$ is shown for different choices of the time interval Δt_c between two successive abrupt changes of desorption. Several horizontal arrows are inserted in Fig. 4 and placed at certain values of the coverage θ in the range [0.890, 0.955]. These arrows show how much more time is needed for a system to reach a given coverage θ in the case when the desorption probability has the constant value $P_{des}^{min}(\theta)$ in time (for comparison, see Fig. 3). For coverages above $\theta \approx 0.92$ these differences are greater than 50%.

The interpretation of these results is quite straightforward using the results of [18,20,28,29]. At a certain time t_0, desorption probability changes from $P_{des}^{(1)}$ to another value $P_{des}^{(2)} = P_{des}^{(1)} - \Delta P_{des}$. For $P_{des}^{(1)} > P_{des}^{(2)}$ we find that the

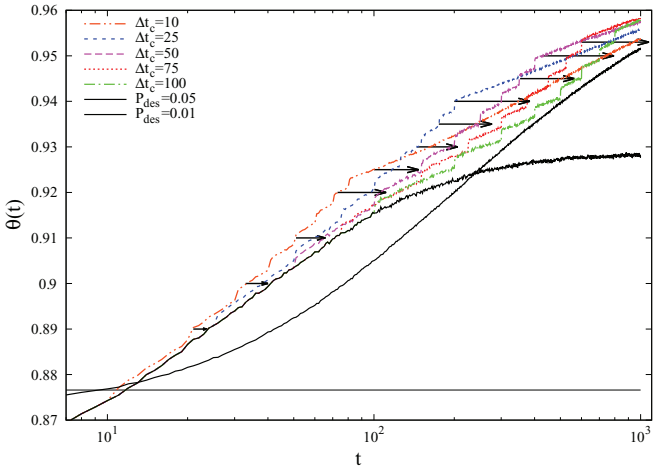

FIG. 4. (Color online) Temporal behavior of the coverage $\theta(t)$ when the desorption probability $P_{\rm des}$ decreases from $P_{\rm des}^{(I)} = 0.050$ to $P_{\rm des}^{(F)} = 0.010$ in a stepwise manner. The desorption probability is abruptly lowered by $\Delta P_{\rm des} = 0.005$ at fixed time intervals $\Delta t_c =$ 10, 25, 50, 75, 100, as indicated in the legend. Vertical coordinates of arrows are $\theta = 0.953$, 0.950, 0.945, 0.940, 0.935, 0.930, 0.925, 0.920, 0.91, 0.9, 0.89, from top to bottom. Arrows show how much more time is needed for a system to reach the given coverage θ in the case when desorption probability has the constant value $P_{\rm des}^{\rm min}(\theta)$ in time (e.g., see Fig. 3). The horizontal line represents the jamming coverage for dimers, $\theta_{\rm jam} = 0.8766$.

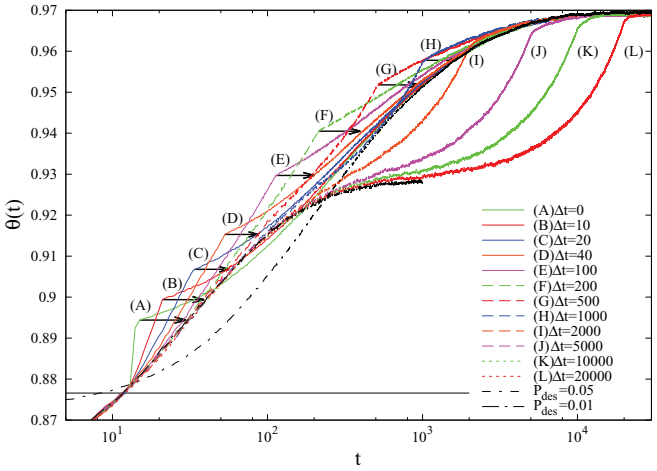

FIG. 5. (Color online) Temporal behavior of the coverage $\theta(t)$ when the desorption probability $P_{\rm des}$ decreases linearly with time from $P_{\rm des}^{(I)} = 0.050$ to $P_{\rm des}^{(F)} = 0.010$. The final probability of $P_{\rm des}^{(2)}$ is reached during the time interval Δt. Curves (A)–(L) correspond to various time intervals Δt ranging from 0 to 2×10^4, as indicated in the legend. Vertical coordinates of arrows are $\theta = 0.9578$(H), 0.9518(G), 0.9405(F), 0.9297(E), 0.9153(D), 0.9068(C), 0.8994(B), 0.8944(A), from top to bottom. Arrows show how much more time is needed for a system to reach the given coverage θ in the case when desorption probability has the constant value $P_{\rm des}^{\rm min}(\theta)$ in time (e.g., see Fig. 3). The horizontal line represents the jamming coverage for dimers, $\theta_{\rm jam} = 0.8766$.

compaction rate increases on short-time scales (Fig. 4). Note that for $P_{\rm des}^{(1)} < P_{\rm des}^{(2)} = P_{\rm des}^{(1)} + \Delta P_{\rm des}$ we observe a short-term effect opposite to the previous case [18,20]. The compaction rate just before t_0 is determined by the desorption probability $P_{\rm des}(t_0 - 0)$ and by the fraction of the substrate, $\Phi(t_0 - 0)$, that is available for the insertion of a new particle. The quantity $\Phi(t_0 - 0)$ (the insertion probability) strongly depends on the state of the system, but it is not unambiguously determined by the coverage fraction $\theta(t_0 - 0)$ at the same instant [18,20]. When $P_{\rm des}$ is abruptly lowered, the first effect is that the particles tend to decrease the fraction of the substrate that is available for deposition of new particles, and the layer becomes more compact. Therefore the rate of compaction first increases with respect to the unperturbed case. At larger times, however, the compaction is slowed down by the creation of a denser substrate and smaller fraction of the layer that is available for the insertion of a new particle.

B. Linear decrease of the desorption probability $P_{\rm des}$

The comparison of the coverage relaxations at various abrupt changes in the desorption probability shows that the amplitude of the jump in the compaction rate is larger for a larger jump of desorption probability [20]. However, it is important to consider the case when the desorption probability varies continuously over a certain time domain. Here we show that the linear decay in the desorption probability as a function of time may be used to hasten the deposition process.

Similar to the procedure described in Sec. III A, the system first evolves at a fixed desorption probability $P_{\rm des}^{(1)}$, up to the intersection point of relaxation curves, corresponding to the coverage $\theta^{(1)} \approx 0.8783 > \theta_{\rm jam}$ at time $t_1 = 12$ (see Fig. 1). Then, the desorption probability starts to decrease linearly with time according to $P_{\rm des}(t) = K(t - t_1) + P_{\rm des}^{(1)}$, where $t_1 < t < t_2$. The final probability of $P_{\rm des}^{(2)}$ is reached during the time interval $\Delta t = t_2 - t_1$, so that the negative slope coefficient $K = -(P_{\rm des}^{(1)} - P_{\rm des}^{(2)})/(t_2 - t_1) = -\Delta P_{\rm des}/\Delta t$ depends on the time interval Δt. In Fig. 5 the temporal dependence of coverage $\theta(t)$ is displayed for the fixed probabilities $P_{\rm des}^{(1)} = 0.050$ and $P_{\rm des}^{(2)} = 0.010$, and for different time intervals $\Delta t = 0, 10, 20, 40, 100, 200, 500, 10^3, 2 \times 10^3, 5 \times 10^3, 10^4, 2 \times 10^4$. Several horizontal arrows are placed at certain values of coverage θ in order to show that much more time is needed for a system to reach a given coverage θ in the case when the desorption probability has a constant value $P_{\rm des}^{\rm min}(\theta)$ in time (e.g., see Fig. 3).

The starting points of horizontal vectors in Fig. 5 are located at points (A)–(H) where the linear decrease of probability $P_{\rm des}(t)$ stops. The envelope containing the points (A)–(H) determines the minimal times $t_\theta^{\rm min}$ needed for a system to reach the given coverages θ, provided that the probability $P_{\rm des}(t)$ decreases linearly in time. These minimal times $t_\theta^{\rm min}$ are shown in Fig. 6 for the reversible deposition process with linear decrease of desorption probability from $P_{\rm des}^{(1)} = 0.050$ to $P_{\rm des}^{(2)} = 0.010$ during the corresponding time intervals Δt. Figure 6 shows that the process of achieving the coverages that are close to the stationary coverage $\theta_\infty(P_{\rm des}^{(2)}) \approx 0.97$ is not possible to speed up significantly by linear decreasing of the desorption probability. In other words, the time needed for a system to reach coverages greater than $\theta(H) \approx 0.9578$ cannot be reduced further by increasing the time interval Δt (see Fig. 6).

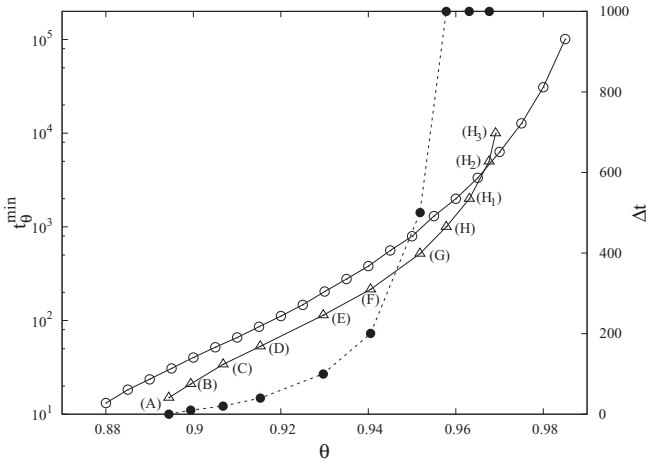

FIG. 6. Plot of the minimal time $t_\theta^{\min}$ (empty triangles) needed for a system to reach a given coverage θ in the reversible deposition process with linear decrease of desorption probability $P_{\rm des}$ from $P_{\rm des}^{(1)} = 0.050$ to $P_{\rm des}^{(2)} = 0.010$ during the time interval Δt. The full symbols are plotted against the right-hand axis and give the time intervals Δt which correspond to densities at points (A)–(H), (H_1), (H_2), and (H_3). For comparison, empty circles correspond to the minimal time $t_\theta^{\min}$ for a system to reach the given coverage θ in the reversible deposition process with a constant value of desorption probability $P_{\rm des}^{\min}(\theta)$ (e.g., see Fig. 3).

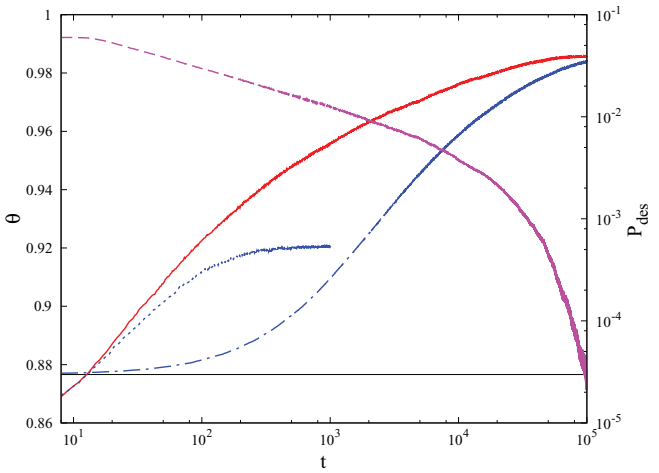

FIG. 7. (Color online) Shown here is the time dependence of the coverage fraction θ in the case of density controlled desorption probability $P_{\rm des}(t) = P_{\rm des}^{\min}(\theta(t))$ (red, solid line, left-hand axis). The dependence of probability $P_{\rm des}^{\min}(\theta)$ on the density θ is shown in Fig. 3. Dotted and dash-dotted (blue) lines represent the results obtained for $P_{\rm des} = 0.060$ and 0.001, respectively. The dashed (magenta) line is plotted against the right-hand axis and gives the numerically obtained temporal behavior of desorption probability $P_{\rm des}(t)$. The horizontal line represents the jamming coverage for dimers, $\theta_{\rm jam} = 0.8766$.

C. Density controlled desorption probability $P_{\rm des}$

We now introduce a protocol for reversible RSA which optimizes the deposition process. Here we do not impose any assumption on the time dependence of desorption probability $P_{\rm des}$, but the probability $P_{\rm des}$ is determined by the current value of density $\theta(t)$ that is reached during the process. In the case of deposition with a constant value of desorption probability, we determined probabilities $P_{\rm des}^{\min}(\theta)$ needed for the system to reach a given coverage $\theta > \theta_{\rm jam}$ in the shortest period of time $t_\theta^{\min}$. These results are shown in Fig. 3, where the solid line represents the exponential fit of the form $P_{\rm des}^{\min}(\theta) = P_1 + P_2 \exp(-\lambda\theta)$, with $P_1 = -5.915 \times 10^{-2}$, $P_2 = 32.30$, and $\lambda = 6.393$. The deposition procedure consists in first achieving the density θ just above the jamming density $\theta_{\rm jam}$ by using the constant desorption probability. Then, the desorption probability $P_{\rm des}$ is reduced during the deposition process in accordance with the exponential dependence of probability $P_{\rm des}^{\min}(\theta)$ on the density θ shown in Fig. 3. In addition, the corresponding dependence of the desorption probability on the time $P_{\rm des}(t)$ can be obtained from numerical simulation.

The simulation corresponding to the described protocol has been run for the initial desorption probability $P_{\rm des} = 0.060$. In Fig. 7 the temporal dependence of coverage $\theta(t)$ is displayed for times $t < 10^5$. For comparison, we also plot the temporal dependence of coverage $\theta(t)$ for the fixed probabilities, $P_{\rm des} = 0.060$, 0.001. It should be noticed that the coverage growth for the deposition process realized using this protocol is much faster than the growth for the constant desorption case. Also, this growth is much faster at the beginning of the process. In the same figure, the corresponding desorption probability $P_{\rm des}$ is plotted as a function of time on a log-log scale. Initially, the desorption probability decreases algebraically in time, but the late-time changes in desorption probability become very small.

For comparison, Fig. 8 includes numerical values of time needed for a system to reach a given coverage $\theta > \theta_{\rm jam}$ in the case of the deposition protocol discussed above, and in the case of reversible RSA with constant value of desorption probability $P_{\rm des}^{\min}(\theta)$. The new protocol significantly hastens the process for achieving high coverages. As mentioned in

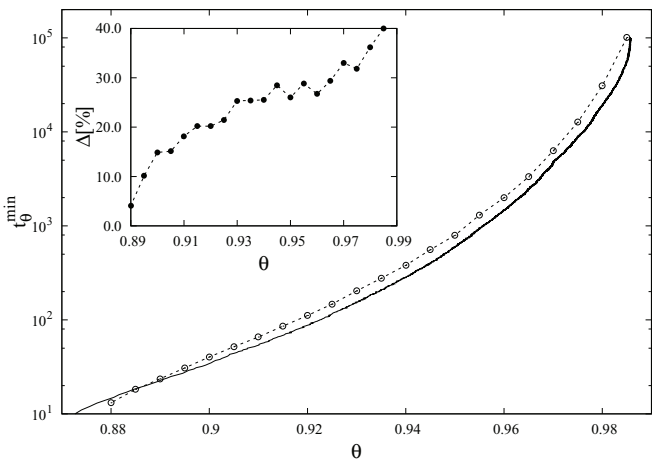

FIG. 8. The solid line represents the time needed for a system to reach a given coverage $\theta > \theta_{\rm jam}$ in the case of deposition process with density controlled desorption probability $P_{\rm des}(t) = P_{\rm des}^{\min}(\theta(t))$ (see Fig. 7). For comparison, we present the minimal time $t_\theta^{\min}$ (empty circles) needed for a system to reach the given coverage θ in the reversible deposition process with a constant value of desorption probability $P_{\rm des}^{\min}(\theta)$ (see Fig. 3). The protocol hastens the deposition process and the corresponding relative decrease Δ in time needed for a system to reach a given coverage θ is shown in the inset.

Sec. III B, the process for achieving high coverages $\theta \gtrsim 0.97$ is not possible to hasten by linear decrease of the desorption probability. Using the above protocol, the times needed for a system to reach the coverages θ in the range (0.965,0.985) are reduced by 29–40%; for coverages $\theta \in (0.93,0.96)$, the times are reduced by 25% (see inset of Fig. 8).

IV. CONCLUSION AND PERSPECTIVES

We have investigated numerically the kinetics of the deposition process of dimers on a 1D lattice in the presence of desorption. A systematic approach is made by examining deposition with various time dependencies of the desorption probability $P_{\rm des}$. We focused on the time evolution of the coverage $\theta(t)$ in the whole postjamming time range $\theta(t) > \theta_{\rm jam}$. In the case of deposition with a constant value of desorption probability, we determined the $P_{\rm des}$ dependence of the time t_θ needed for a system to reach a given coverage $\theta > \theta_{\rm jam}$. Reducing the probability $P_{\rm des}$, the time t_θ may become arbitrarily large, i.e., time t_θ diverges algebraically when $P_{\rm des}$ gets smaller. For each coverage $\theta > \theta_{\rm jam}$, there is the minimal time $t_\theta^{\rm min}$ needed for a system to reach the given coverage θ. For the densities slightly above the jamming coverage $\theta_{\rm jam}$, it is found that the minimal time $t_\theta^{\rm min}$ increases exponentially with density. At high densities, we found that the increase of $t_\theta^{\rm min}$ with density is faster than exponential (see, Fig. 3). Minimal time $t_\theta^{\rm min}$ is expected to diverge at the maximal close packing $\theta = 1$.

We have shown that the time needed for a system to reach a given coverage θ may be less than $t_\theta^{\rm min}$ if $P_{\rm des}$ decreases in time. We have considered the behavior of the system when the desorption probability $P_{\rm des}$ decreases both stepwise and linearly (continuously) over a certain time domain. Furthermore, the initial and final desorption probability do not have arbitrary values. If $P_{\rm des}$ is large enough, the system will not reach the jamming. In other words, there is an upper limit $P_{\rm des}^B$ of the desorption probability, above which the steady-state coverage will be lower than the jamming limit. For our 1D system we use $P_{\rm des}^B \approx 0.10$. The greatest impact on the deposition rate is obtained if the initial value of the desorption probability $P_{\rm des}^{(I)}$ corresponds to the limiting value $P_{\rm des}^B$. The final value of the desorption probability $P_{\rm des}^{(F)}$ determines the maximal value of the coverage $\theta_\infty(P_{\rm des}^{(F)})$ that can be achieved. We have shown that for each coverage fraction θ between $\theta_{\rm jam}$ and $\theta_\infty(P_{\rm des}^{(F)})$, there is an optimal rate K for the linear decrease of $P_{\rm des}(t)$ when the time needed for a system to reach the given coverage θ is minimal. Finally, a self-consistent optimization procedure for reversible RSA is formulated and tested. In this case, the probability $P_{\rm des}$ is determined by the current coverage density $\theta(t)$. This value is chosen as the probability that gives minimal time needed for a system to reach the current coverage $\theta(t)$ in the constant desorption case. Our protocol significantly hastens the process for achieving high coverage densities.

Since the time needed for a system to reach a given coverage θ can be significantly reduced if $P_{\rm des}$ decreases in time, we propose the application of an analog procedure to optimize the compaction process in weakly vibrated granular materials. Granular materials are complex systems exhibiting rich macroscopic phenomenology and showing many characteristic glassy behaviors. One of the striking features of granular materials are the memory effects observed by measuring the short-time response to an instantaneous change in tapping acceleration Γ [30]. For a sudden decrease in Γ it was observed that on short-time scales the compaction rate increases, while for a sudden increase in Γ the system dilates for short times. This behavior is transient and after several taps there is a crossover to the "normal" behavior, with the relaxation rate becoming the same as in constant vibration intensity mode. The short-term memory effects observed in granular materials are reflected in the fact that the future evolution of the packing fraction θ after time t_0 depends not only on the $\theta(t_0)$, but also on the previous tapping history. Response properties of granular media and the observation of short-term memory effects indicate that the change in tapping acceleration Γ can affect the dynamics and efficiency of the compaction process.

It is important to note that the parking lot model (PLM, 1D off-lattice reversible RSA model) [17,18,29] is a widely used model which can reproduce qualitatively the densification kinetics and other features of a weakly vibrated granular material. The dynamics of both the present model and the PLM depends essentially on the excluded volume and geometrical frustration. Therefore, one would expect that the growth of the coverage in the case of the PLM can also be accelerated by decreasing the desorption rate during the deposition process. The presented numerical analysis could be a first step toward dealing with more realistic situations, such as the case of compaction of a granular assembly of spheres under variable intensity of external excitations (e.g., tapping, periodic shear deformation, thermal cycling). However, any numerical treatment of this problem by molecular dynamics [31] is necessarily very time consuming and is beyond the scope of this paper.

ACKNOWLEDGMENT

This work was partially supported by the MESTDRS, under Grants No. ON171017 and No. III45016.

[1] J. W. Evans, Rev. Mod. Phys. **65**, 1281 (1993).
[2] *Adhesion of Submicron Particles on Solid Surfaces*, edited by V. Privman, Colloids Surf. A **165**, 1 (2000).
[3] A. Cadilhe, N. A. M. Araújo, and V. Privman, J. Phys.: Condens. Matter **19**, 065124 (2007).
[4] J. Feder, J. Theor. Biol. **87**, 237 (1980).
[5] R. H. Swendsen, Phys. Rev. A **24**, 504 (1981).
[6] Y. Pomeau, J. Phys. A: Math. Gen. **13**, L193 (1980).
[7] B. Bonnier, Phys. Rev. E **64**, 066111 (2001).
[8] M. C. Bartelt and V. Privman, J. Chem. Phys. **93**, 6820 (1990).
[9] P. Nielaba, V. Privman, and J. S. Wang, J. Phys. A: Math. Gen. **23**, L1187 (1990).

[10] S. S. Manna and N. M. Švrakić, J. Phys. A: Math. Gen. **24**, L671 (1991).
[11] Lj. Budinski-Petković and U. Kozmidis-Luburić, Phys. Rev. E **56**, 6904 (1997).
[12] Lj. Budinski-Petković and U. Kozmidis-Luburić, Physica A **236**, 211 (1997).
[13] P. L. Krapivsky and E. Ben-Naim, J. Chem. Phys. **100**, 6778 (1994).
[14] Lj. Budinski-Petković and U. Kozmidis-Luburić, Physica A **301**, 174 (2001).
[15] I. Lončarević, Lj. Budinski-Petković, S. B. Vrhovac, and A. Belić, Phys. Rev. E **80**, 021115 (2009).
[16] Lj. Budinski-Petković, M. Petković, Z. M. Jakšić, and S. B. Vrhovac, Phys. Rev. E **72**, 046118 (2005).
[17] A. J. Kolan, E. R. Nowak, and A. V. Tkachenko, Phys. Rev. E **59**, 3094 (1999).
[18] J. Talbot, G. Tarjus, and P. Viot, Phys. Rev. E **61**, 5429 (2000).
[19] G. Tarjus and P. Viot, Phys. Rev. E **69**, 011307 (2004).
[20] Lj. Budinski-Petković and S. B. Vrhovac, Eur. Phys. J. E **16**, 89 (2005).
[21] P. Richard, M. Nicodemi, R. Delannay, P. Ribière, and D. Bideau, Nat. Mater. **4**, 121 (2005).
[22] J. B. Knight, C. G. Fandrich, C. N. Lau, H. M. Jaeger, and S. R. Nagel, Phys. Rev. E **51**, 3957 (1995).
[23] F. X. Villarruel, B. E. Lauderdale, D. M. Mueth, and H. M. Jaeger, Phys. Rev. E **61**, 6914 (2000).
[24] P. Philippe and D. Bideau, Europhys. Lett. **60**, 677 (2002).
[25] P. Ribière, P. Richard, D. Bideau, and R. Delannay, Eur. Phys. J. E **16**, 415 (2005).
[26] P. Ribière, P. Richard, P. Philippe, D. Bideau, and R. Delannay, Eur. Phys. J. E **22**, 249 (2007).
[27] R. S. Ghaskadvi and M. Dennin, Phys. Rev. E **61**, 1232 (2000).
[28] J. Talbot, G. Tarjus, and P. Viot, J. Phys. A: Math. Gen. **32**, 2997 (1999).
[29] J. Talbot, G. Tarjus, and P. Viot, Eur. Phys. J. E **5**, 445 (2001).
[30] C. Josserand, A. Tkachenko, D. M. Mueth, and H. M. Jaeger, Phys. Rev. Lett. **85**, 3632 (2000).
[31] D. Arsenović, S. B. Vrhovac, Z. M. Jakšić, L. Budinski-Petković, and A. Belić, Phys. Rev. E **74**, 061302 (2006).